Supporting Information for

Thermal conductivity and balanced performance in infrared nonlinear optical multicomponent chalcogenides $Li_xAg_{1-x}Ga_yIn_{1-y}Se_2$

L.I. Isaenko [a,c,], Bohui Xu [b,d], K.E. Korzhneva [a], Pifu Gong [b], D.A. Samoshkin [e], A.F. Kurus [a,c], Zheshuai Lin [b,d,*]*

a. Sobolev Institute of Geology and Mineralogy SB RAS, Novosibirsk 630090 Russia
Email: lyudmila.isaenko@mail.ru (L. I.)
b. Functional Crystals Lab, Technical Institute of Physics and Chemistry, Chinese Academy of Sciences, Beijing 100190, China
Email: zslin@mail.ipc.ac.cn
c. Novosibirsk State University, Novosibirsk 630090 Russia
d. Centre of Materials Science and Optoelectronics Engineering, University of Chinese Academy of Sciences, Beijing 100049, China
e. Kutateladze Institute of Thermophysics SB RAS, Novosibirsk 630090, Russia

*Corresponding author

List of Contents

Figure S3. Phonon desperation curve and phonon DOS of (a) $LiGaSe_2$, (b) $LiAgGa_2Se_4$, (c) $AgGaSe_2$.

1. Experimental method

1.1. Theoretical calculations

All values of the lattice heat capacity k_L at 300 K used for ML modeling with TL-CGCNN algorithm were obtained using data from Ref. [1-4],[1-4] containing not only CIF structural files, but also certain basic properties of solid solutions both calculated using the PBE functional and obtained experimentally. TL-CGCNN algorithm offers instant and high-performance k_L research with a small expenditure of machine time. Our previous study has determined reliable computational parameters for the TL-CGCNN algorithm in convolutional neural network of ML model, which were used for high-performance screening and pre-experimental design on the NLO chalcogenides with high thermal conductivity.[5] The TLC GC model was used to predict the thermal conductivity of elementary compounds, assuming symmetrical positions of *A* and *B* in the ABC_2 system. For $AgGa_yIn_{1-y}Se_2$, the *A*-position is fixed as Ag and the ratio of Ga/In units in the *B*-position is controlled. The model of high-performance screening and pre-experimental design were considered in Ref. [6]. Density functional theory implemented in the CASTEP package[6] is used to calculate the SHG coefficients, energy band gaps and birefringence values in our studied multicomponent chalcogenides, and the computational details are presented in Ref. [7]. [7]

1.2. Measurement of thermal conductivity

A non-stationary short-term heating method, i.e., the laser flash method, is used to directly measure temperature conductivity k_T, which a physical parameter characterizes the rate of change (equalization) of the temperature of a substance in nonequilibrium thermal processes. Consequently, the thermal conductivity *k* of the studied material can be determined by taking into account the known values of the specific heat capacity C_p and density ρ, as well as k_T, using the formula $k = k_T \cdot C_p \cdot \rho$. [8]

The laser flash measurements at a given temperature *T* are carried out in a series of two laser "flashes" with the interval of 3 minutes after thermostating the sample on an automated LFA-427 device from NETZSCH (Germany) in an atmosphere of high-purity argon (99.992) in the temperature range 23-300 °C. The interval between the "flashes" was 3 minutes. The description of the measurement method and the experimental setup are represented in Ref.

[8] and [9].[8, 9] It is important to note that all samples had the same thickness, since thickness is an important parameter for the laser "flash" method.

Based on the laser flash method, we determine the thermal conductivity of $LiInSe_2$, $LiGaSe_2$, $Li_{0.8}Ag_{0.2}InSe_2$, $Li_{0.5}Ag_{0.5}GaSe_2$, $AgGaSe_2$, $AgInSe_2$ crystals. **Table S1** shows the values of thermal conductivity, heat capacity and density of the listed crystals. In Ref. [10],[10] experimental data of measuring the heat capacity of $LiInS_2$, $LiInSe_2$, $LiGaS_2$, $LiGaSe_2$ and $LiGaTe_2$ crystals in the temperature range from 180 to 460 K were obtained. The thermal conductivity values for $AgGaSe_2$ and $AgInSe_2$ are taken from other sources. [1, 2]

Table S1. Heat capacity, density and thermal conductivity for $LiGaSe_2$, $LiInSe_2$, $Li_{0.8}Ag_{0.2}InSe_2$, $Li_{0.5}Ag_{0.5}GaSe_2$, $AgGaSe_2$ and $AgInSe_2$

Crystal	Heat capacity, J/g*K	Density, g/cm^3	Thermal conductivity, W/m*K
$LiGaSe_2$	0.41 [10]	4.21 [11]	4.57 [11]
$LiInSe_2$	0.34 [10]	4.47 [12]	4.9 [13]
$Li_{0.5}Ag_{0.5}GaSe_2$	0.34 (exp.)	4.69 (exp.)	1.23 (exp.)
$Li_{0.8}Ag_{0.2}InSe_2$	0.33 (exp.)	4.48 (exp.)	2.1 (exp.)
$AgGaSe_2$	0.29 [1]	5.68 [14]	1.1 [15]
$AgInSe_2$	0.26 [2]	5.84 [16]	0.99 [17]

Table S2. Lattice thermal conductivity (k_L), nonlinearity coefficient (d_{ij}) and band gap (*Eg*) for solid solutions $Li_xAg_{1-x}GaSe_2$ and $Li_xAg_{1-x}InSe_2$

Solid solution	Composition	Space group	k_L, $W*m^{-1}*K^{-1}$		d_{ij}, $pm*V^{-1}$	Eg, eV
			cal.	exp.		
$Li_xAg_{1-x}GaSe_2$	$AgGaSe_2$	*I*-42*d*	0.99	1.1 [16]	39.5	1.8
	$Li_{0.125}Ag_{0.865}GaSe_2$	*I*-42*d*	1.09			
	$Li_{0.25}Ag_{0.75}GaSe_2$	*I*-42*d*	1.37			
	$Li_{0.5}Ag_{0.5}GaSe_2$	*I*-42*d*	2.14	1.23	26	2.11
	$Li_{0.6}Ag_{0.4}GaSe_2$	*I*-42*d*	2.57		38	2.08
	$Li_{0.8}Ag_{0.2}GaSe_2$	*I*-42*d*	3.06		43	2.22
	$Li_{0.9}Ag_{0.1}GaSe_2$	*I*-42*d*	3.61		31	2.28
	$Li_{0.98}Ag_{0.02}GaSe_2$	$Pna2_1$	3.24			
	$LiGaSe_2$	$Pna2_1$	4.51	4.57 [11]	9.9	3.47
$Li_xAg_{1-x}InSe_2$	$AgInSe_2$	*I*-42*d*	0.96	0.99 [17]	37	1.22
	$Li_{0.2}Ag_{0.8}InSe_2$	*I*-42*d*	1.42		14.47	1.41
	$Li_{0.37}Ag_{0.63}InSe_2$	*I*-42*d*	1.69		21.8	
	$Li_{0.55}Ag_{0.45}InSe_2$	$Pna2_1$	2.21		17.6	1.92
	$Li_{0.78}Ag_{0.22}InSe_2$	$Pna2_1$	3.06		28.8	2.2
	$Li_{0.81}Ag_{0.19}InSe_2$	$Pna2_1$	3.41		26.3	2.27
	$LiInSe_2$	$Pna2_1$	4.6	4.9 [15]	11.7	2.86

Table S3. Lattice thermal conductivity (k_L) for solid solution $AgGa_yIn_{1-y}Se_2$

Composition	Space group	k_L, $W*m^{-1}*K^{-1}$	
		cal	exp
$AgInSe_2$	*I*-42*d*	0.96	0.99 [17]
$AgGa_{0.2}In_{0.8}Se_2$	*I*-42*d*	0.93	
$AgGa_{0.4}In_{0.6}Se_2$	*I*-42*d*	0.91	
$AgGa_{0.5}In_{0.5}Se_2$	*I*-42*d*	0.89	
$AgGa_{0.665}In_{0.335}Se_2$	*I*-42*d*	0.94	
$AgGa_{0.82}In_{0.18}Se_2$	*I*-42*d*	0.93	
$AgGaSe_2$	*I*-42*d*	0.99	1.1 [16]

Table S4. Molecular weight and average Li(Ag)-Se or Ga(In)-Se bond lengths for $Li_xAg_{1-x}GaSe_2$, $Li_xAg_{1-x}InSe_2$ and $AgGa_yIn_{1-y}Se_2$ solid solutions

Solid solution	Composition	Space group	Molecular weight, a.e.m.	Bond lenght Li(Ag)-Se or Ga(In)-Se, Å
$Li_xAg_{1-x}GaSe_2$ [3]	$AgGaSe_2$	*I*-42*d*	335.51	2.6416
	$Li_{0.125}Ag_{0.865}GaSe_2$	*I*-42*d*	321.88	2.5927
	$Li_{0.25}Ag_{0.75}GaSe_2$	*I*-42*d*	310.28	2.5885
	$Li_{0.5}Ag_{0.5}GaSe_2$	*I*-42*d*	285.04	2.5898
	$Li_{0.6}Ag_{0.4}GaSe_2$	*I*-42*d*	274.95	2.5755
	$Li_{0.8}Ag_{0.2}GaSe_2$	*I*-42*d*	254.77	2.5593
	$Li_{0.9}Ag_{0.1}GaSe_2$	*I*-42*d*	244.67	2.5387
	$Li_{0.98}Ag_{0.02}GaSe_2$	$Pna2_1$	236.6	2.5588
	$LiGaSe_2$	$Pna2_1$	234.58	2.5509
$Li_xAg_{1-x}InSe_2$ [4]	$AgInSe_2$	*I*-42*d*	380.61	2.6354
	$Li_{0.2}Ag_{0.8}InSe_2$	*I*-42*d*	360.42	2.6154
	$Li_{0.37}Ag_{0.63}InSe_2$	*I*-42*d*	343.26	2.6039
	$Li_{0.55}Ag_{0.45}InSe_2$	$Pna2_1$	325.1	2.5823
	$Li_{0.78}Ag_{0.22}InSe_2$	$Pna2_1$	301.88	2.5603
	$Li_{0.81}Ag_{0.19}InSe_2$	$Pna2_1$	298.85	2.559
	$LiInSe_2$	$Pna2_1$	279.68	2.5498
$AgGa_yIn_{1-y}Se_2$	$AgGaSe_2$ [3]	*I*-42*d*	335.51	2.6416
	$AgGa_{0.82}In_{0.18}Se_2$ [18]	*I*-42*d*	343.63	2.6105
	$AgGa_{0.665}In_{0.335}Se_2$ [18]	*I*-42*d*	350.62	2.6274
	$AgGa_{0.5}In_{0.5}Se_2$ [19]	*I*-42*d*	358.06	2.59
	$AgGa_{0.4}In_{0.6}Se_2$ [20]	*I*-42*d*	362.57	2.6068
	$AgGa_{0.2}In_{0.8}Se_2$ [20]	*I*-42*d*	371.59	2.6104
	$AgInSe_2$ [4]	*I*-42*d*	380.61	2.6354

Table S5. Electronegativity of atoms, electronegativity difference and the nature of chemical bonding for solid solutions $Li_xAg_{1-x}GaSe_2$, $Li_xAg_{1-x}InSe_2$ and $AgGa_yIn_{1-y}Se_2$

Solid solution	Composition	Electronegativity of atoms (χ), eV	Electronegativity difference (Δχ), eV	The nature of the chemical bond
$Li_xAg_{1-x}GaSe_2$	$AgGaSe_2$	χ(Li)=1, χ(Ag)=1.9, χ(Ga)=1.6, χ(Se)=2.4	1.3	polar covalent
	$Li_{0.125}Ag_{0.865}GaSe_2$		1.43	
	$Li_{0.25}Ag_{0.75}GaSe_2$		1.53	
	$Li_{0.5}Ag_{0.5}GaSe_2$		1.75	
	$Li_{0.6}Ag_{0.4}GaSe_2$		1.84	
	$Li_{0.8}Ag_{0.2}GaSe_2$		2.02	Ionic
	$Li_{0.9}Ag_{0.1}GaSe_2$		2.11	
	$Li_{0.98}Ag_{0.02}GaSe_2$		2.18	
	$LiGaSe_2$		2.2	
$Li_xAg_{1-x}InSe_2$	$AgInSe_2$	χ(Li)=1, χ(Ag)=1.9, χ(In)=1.7, χ(Se)=2.4	1.2	polar covalent
	$Li_{0.2}Ag_{0.8}InSe_2$		1.38	
	$Li_{0.37}Ag_{0.63}InSe_2$		1.53	
	$Li_{0.55}Ag_{0.45}InSe_2$		1.7	
	$Li_{0.78}Ag_{0.22}InSe_2$		1.9	
	$Li_{0.81}Ag_{0.19}InSe_2$		1.93	
	$LiInSe_2$		2.1	Ionic
$AgGa_yIn_{1-y}Se_2$	$AgGaSe_2$ [3]	χ(Ag)=1.9, χ(Ga)=1.6, χ(In)=1.7, χ(Se)=2.4	1.3	polar covalent
	$AgGa_{0.82}In_{0.18}Se_2$ [18]		1.28	
	$AgGa_{0.665}In_{0.335}Se_2$ [18]		1.27	
	$AgGa_{0.5}In_{0.5}Se_2$ [19]		1.25	
	$AgGa_{0.4}In_{0.6}Se_2$ [20]		1.24	
	$AgGa_{0.2}In_{0.8}Se_2$ [20]		1.22	
	$AgInSe_2$ [4]		1.2	

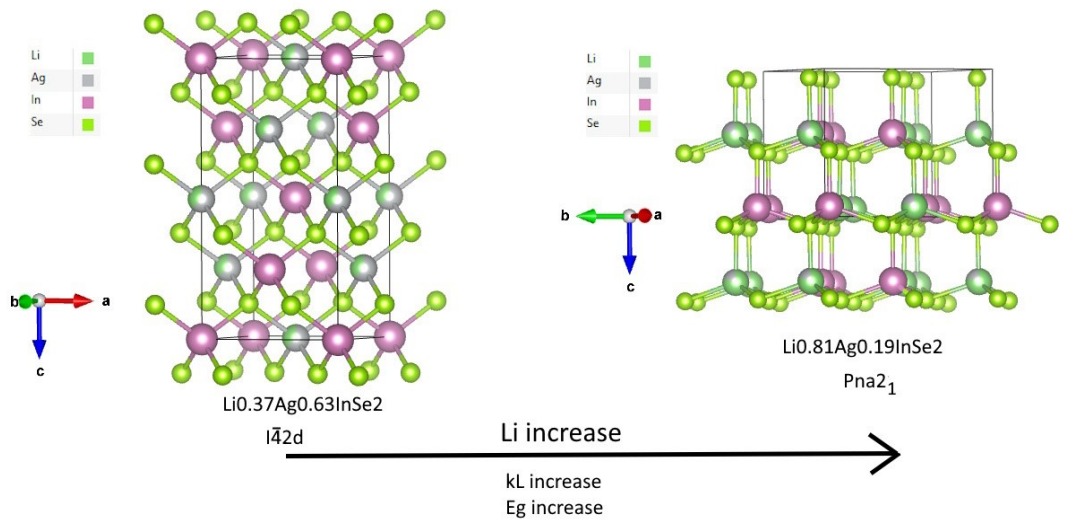

Figure S1. Structure changes from tetragonal (I-42d) to rhombic (Pna21) and the trend of the main features.

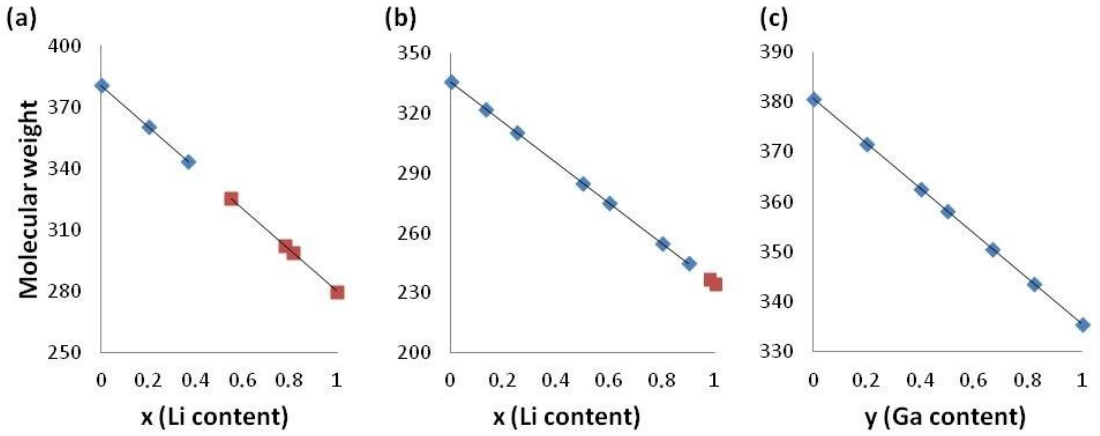

Figure S2. Decrease of molecular weight for solid solutions (a) $Li_xAg_{1-x}InSe_2$, (b) $Li_xAg_{1-x}GaSe_2$, (c) $AgGa_yIn_{1-y}Se_2$.

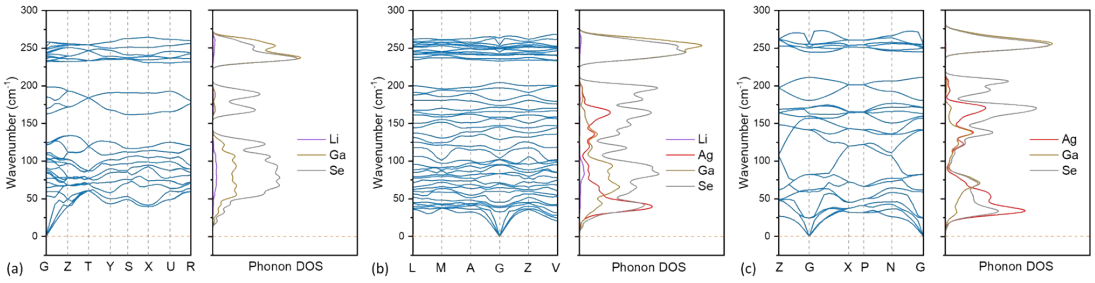

Figure S3. Phonon desperation curve and phonon DOS of (a) $LiGaSe_2$, (b) $LiAgGa_2Se_4$, (c) $AgGaSe_2$.

References

1. H. J. Hou, F. J. Kong, J. W. Yang, L. H. Xie and S. X. Yang, First-principles study of the structural, optical and thermal properties of AgGaSe2, *Phys. Scr.*, 2014, **89**, 065703.
2. H. Neumann, J. Łażewski, P. T. Jochym and K. Parlinski, Ab initio heat capacity and atomic temperature factors of chalcopyrites, *Phys. Rev. B*, 2007, **75**, 224301.
3. L. Isaenko, L. Dong, A. Kurus, Z. Lin, A. Yelisseyev, S. Lobanov, M. Molokeev, K. Korzhneva and A. Goloshumova, $Li_xAg_{1-x}GaSe_2$: Interplay Between Lithium and Silver in Mid-Infrared Nonlinear Optical Chalcogenides, *Adv. Opt. Mater.*, 2022, **10**, 2201727.
4. L. Isaenko, L. Dong, K. Korzhneva, A. Yelisseyev, S. Lobanov, S. Gromilov, M. S. Molokeev, A. Kurus and Z. Lin, Evolution of Structures and Optical Properties in a Series of Infrared Nonlinear Optical Crystals $Li_xAg_{1-x}InSe_2$ ($0 \leq x \leq 1$), *Inorg. Chem.*, 2023, **62**, 15936-15942.
5. Q. Wu, L. Kang and Z. Lin, A Machine Learning Study on High Thermal Conductivity Assisted to Discover Chalcogenides with Balanced Infrared Nonlinear Optical Performance, *Adv. Mater.,* 2024, **36**, 2309675.
6. S. J. Clark, M. D. Segall, C. J. Pickard, P. J. Hasnip, M. I. J. Probert, K. Refson and M. C. Payne, First principles methods using CASTEP, 2005, **220**, 567-570.
7. Z. Lin, X. Jiang, L. Kang, P. Gong, S. Luo and M.-H. Lee, First-principles materials applications and design of nonlinear optical crystals, *J. Phys. D: Appl. Phys.*, 2014, **47**, 253001.
8. W. J. Parker, R. J. Jenkins, C. P. Butler and G. L. Abbott, Flash Method of Determining Thermal Diffusivity, Heat Capacity, and Thermal Conductivity, *J. Appl. Phys.*, 1961, **32**, 1679-1684.
9. I. V. Savchenko and S. V. Stankus, Thermal conductivity and thermal diffusivity of tantalum in the temperature range from 293 to 1800 K, *Thermophys. and Aeromech.*, 2008, **15**, 679-682.
10. V. A. Drebushchak, L. I. Isaenko, S. I. Lobanov, P. G. Krinitsin and S. A. Grazhdannikov, Experimental heat capacity of $LiInS_2$, $LiInSe_2$, $LiGaS_2$, $LiGaSe_2$, and $LiGaTe_2$ from 180 to 460 K, *J. Therm. Anal. Calorim.*, 2017, **129**, 103-108.
11. M. S. Yaseen, G. Murtaza and R. M. Arif Khalil, Ab-initio study of Li based chalcopyrite compounds $LiGaX_2$ (X= S, Se, Te) in tetragonal symmetry: A class of future materials for optoelectronic applications, *Current Applied Physics*, 2018, **18**, 1113-1121.
12. A. Kargar, H. Hong, J. Tower, A. Gueorguiev, H. Kim, L. Cirignano, J. F. Christian, M. R. Squillante and K. Shah, $LiInSe_2$ for Semiconductor Neutron Detectors, 2020, **8**.
13. A. P. Yelisseyev, A. S. Titov, K. M. Lyapunov, V. A. Drebushchak, L. I. Isaenko and S. I. Lobanov, Thermal and thermo-optic parameters of $LiInSe_2$ single crystals, *J. Cryst. Growth*, 2005, **275**, e1679-e1684.
14. R. L. Aggarwal and T. Y. Fan, Thermal diffusivity, specific heat, thermal conductivity, coefficient of thermal expansion, and refractive-index change with temperature in $AgGaSe_2$, *Appl. Opt.*, 2005, **44**, 2673-2677.
15. S. Sharma, A. S. Verma and V. K. Jindal, Ab initio studies of structural, electronic, optical, elastic and thermal properties of silver gallium dichalcogenides ($AgGaX_2$: X=S, Se, Te), *Mater. Res. Bull.*, 2014, **53**, 218-233.
16. H. Hahn, G. Frank, W. Klingler, A.-D. Meyer and G. Störger, Untersuchungen über ternäre Chalkogenide. V. Über einige ternäre Chalkogenide mit Chalkopyritstruktur, 1953, **271**, 153-170.
17. P. Qiu, Y. Qin, Q. Zhang, R. Li, J. Yang, Q. Song, Y. Tang, S. Bai, X. Shi and L. Chen, Intrinsically High Thermoelectric Performance in $AgInSe_2$ n-Type Diamond-Like Compounds, 2018, **5**, 1700727.
18. V. V. Badikov, G. M. Kuz'micheva, V. L. Panyutin, V. B. Rybakov, V. I. Chizhikov, G. S. Shevyrdyaeva and S. I. Shcherbakov, Preparation and Structure of $AgGa_{1-x}In_xSe_2$ Single Crystals, *Inorg. Mater.*, 2003, **39**, 1028-1034.
19. J. E. Avon, K. Yoodee and J. C. Woolley, Solid solution, lattice parameter values, and effects of electronegativity in the $(Cu_{1-x}Ag_x)(Ga_{1-y}In_y)(Se_{1-z}\ Te_z)_2$ alloys, *J. Appl. Phys.*, 1984, **55**, 524-535.
20. S.-R. Hahn and W.-T. Kim, Anomalous composition and temperature dependence of the energy gap of $AgGa_{1-x}In_xSe_2$ mixed crystals, *Phys. Rev. B*, 1983, **27**, 5129-5131.